

# AXIALVECTOR TETRAQUARK CANDIDATES FOR THE $Z_c(3900)$ , $Z_c(4020)$ , $Z_c(4430)$ , $Z_c(4600)$

Zhi-Gang Wang<sup>1</sup>

Department of Physics, North China Electric Power University, Baoding 071003, P. R. China

## Abstract

In this article, we study the ground states and the first radial excited states of the  $Z_c$  tetraquark states with  $J^{PC} = 1^{+-}$  via the QCD sum rules systematically, and observe that there are one axialvector tetraquark candidate for the  $Z_c(3900)$  and  $Z_c(4430)$ , two axialvector tetraquark candidates for the  $Z_c(4020)$ , three axialvector tetraquark candidates for the  $Z_c(4600)$ .

PACS number: 12.39.Mk, 12.38.Lg

Key words: Tetraquark state, QCD sum rules

## 1 Introduction

Recently, the LHCb collaboration performed an angular analysis of the  $B^0 \rightarrow J/\psi K^+ \pi^-$  decays using proton-proton collision data, studied the  $m(J/\psi \pi^-)$  versus  $m(K^+ \pi^-)$  plane, and observed two possible structures near  $m(J/\psi \pi^-) = 4200$  MeV and 4600 MeV, respectively [1]. There have been two tentative assignments of the structure  $Z_c(4600)$  near  $m(J/\psi \pi^-) = 4600$  MeV, the  $[dc]_P[\bar{u}\bar{c}]_A - [dc]_A[\bar{u}\bar{c}]_P$  vector tetraquark state with  $J^{PC} = 1^{--}$  [2] and the first radial excited  $[dc]_T[\bar{u}\bar{c}]_A - [dc]_A[\bar{u}\bar{c}]_T$  tetraquark state with  $J^{PC} = 1^{+-}$  [3]. In this article, we use the subscripts  $S$ ,  $P$ ,  $V$ ,  $A$  and  $T$  to denote the scalar, pseudoscalar, vector, axialvector and tensor diquark states, respectively.

In 2013, the BESIII collaboration observed a structure  $Z_c(3900)$  in the  $\pi^\pm J/\psi$  mass spectrum with a mass of  $(3899.0 \pm 3.6 \pm 4.9)$  MeV and a width of  $(46 \pm 10 \pm 20)$  MeV, respectively [4]. The  $Z_c(3900)$  was also observed by the Belle collaboration [5] and was confirmed by the CLEO collaboration [6]. Also in 2013, the BESIII collaboration observed the  $Z_c^\pm(4025)$  near the  $(D^* \bar{D}^*)^\pm$  threshold in the process  $e^+ e^- \rightarrow (D^* \bar{D}^*)^\pm \pi^\mp$  [7]. Furthermore, the BESIII collaboration observed the  $Z_c^\pm(4020)$  in the  $\pi^\pm h_c$  mass spectrum in the process  $e^+ e^- \rightarrow \pi^+ \pi^- h_c$  [8]. The  $Z_c(4020)$  and  $Z_c(4025)$  are taken as the same particle in The Review of Particle Physics [9]. In 2014, the LHCb collaboration studied the  $B^0 \rightarrow \psi' \pi^- K^+$  decays by performing a four-dimensional fit of the decay amplitude, and provided the first independent confirmation of the existence of the  $Z_c(4430)^-$  state and established its spin-parity to be  $1^+$  [10]. In 2017, the BESIII collaboration determined the spin and parity of the  $Z_c(3900)$  state to be  $J^P = 1^+$  with a statistical significance larger than  $7\sigma$  over other quantum numbers [11].

The  $Z_c(3900)$  and  $Z_c(4430)$  can be assigned to be the ground state and the first radial excited state respectively according to the analogous decays,  $Z_c(3900)^\pm \rightarrow J/\psi \pi^\pm$ ,  $Z_c(4430)^\pm \rightarrow \psi' \pi^\pm$ , and the mass gaps  $M_{Z(4430)} - M_{Z(3900)} \approx m_{\psi'} - m_{J/\psi}$  [12, 13]. In Ref.[14], we apply the approach suggested in Ref.[15] for the quarkonium to study the  $Z_c(3900)$  and  $Z_c(4430)$  as the ground state and the first radial excited state of the axialvector hidden-charm tetraquark states, respectively, and use the energy scale formula  $\mu = \sqrt{M_{X/Y/Z}^2 - (2\mathbb{M}_c)^2}$  with the effective  $c$ -quark mass  $\mathbb{M}_c$  to determine the ideal energy scales of the QCD spectral densities [16]. In Ref.[17], this subject is studied in another QCD sum rules approach. In Refs.[18, 19], we observe that the  $Z_c(4020/4025)$  can be assigned to be the ground state  $[uc]_A[\bar{d}\bar{c}]_A$  tetraquark state with  $J^{PC} = 1^{+-}$  based on the QCD sum rules. If the  $Z_c(4600)$  is the first radial excited state of the  $Z_c(4020/4025)$ , its preferred decay mode is  $Z_c(4600) \rightarrow \psi' \pi$  rather than  $Z_c(4600) \rightarrow J/\psi \pi$ .

In this article, we intend to perform a detailed and updated analysis of the ground states and the first radial excited states of the  $Z_c$  states with the QCD sum rules, and explore the

<sup>1</sup>E-mail: zgwang@aliyun.com.

possible assignments of the  $Z_c(4600)$  state in the scenario of the axialvector tetraquark states with  $J^{PC} = 1^{+-}$ .

The article is arranged as follows: we obtain the QCD sum rules for the axialvector  $Z_c$  states in section 2; we present the numerical results and discussions in section 3; section 4 is reserved for our conclusion.

## 2 The QCD sum rules for the axialvector tetraquark states

We write down the two-point correlation functions  $\Pi_{\mu\nu}(p)$  and  $\Pi_{\mu\nu\alpha\beta}(p)$  in the QCD sum rules,

$$\begin{aligned}\Pi_{\mu\nu}(p) &= i \int d^4x e^{ip \cdot x} \langle 0 | T \{ J_\mu(x) J_\nu^\dagger(0) \} | 0 \rangle, \\ \Pi_{\mu\nu\alpha\beta}(p) &= i \int d^4x e^{ip \cdot x} \langle 0 | T \{ J_{\mu\nu}(x) J_{\alpha\beta}^\dagger(0) \} | 0 \rangle,\end{aligned}\quad (1)$$

where  $J_\mu(x) = J_\mu^1(x), J_\mu^2(x), J_\mu^3(x)$ ,

$$\begin{aligned}J_\mu^1(x) &= \frac{\varepsilon^{ijk}\varepsilon^{imn}}{\sqrt{2}} \left[ u^{Tj}(x) C \gamma_5 c^k(x) \bar{d}^m(x) \gamma_\mu C \bar{c}^{Tn}(x) - u^{Tj}(x) C \gamma_\mu c^k(x) \bar{d}^m(x) \gamma_5 C \bar{c}^{Tn}(x) \right], \\ J_\mu^2(x) &= \frac{\varepsilon^{ijk}\varepsilon^{imn}}{\sqrt{2}} \left[ u^{Tj}(x) C \sigma_{\mu\nu} \gamma_5 c^k(x) \bar{d}^m(x) \gamma^\nu C \bar{c}^{Tn}(x) - u^{Tj}(x) C \gamma^\nu c^k(x) \bar{d}^m(x) \gamma_5 \sigma_{\mu\nu} C \bar{c}^{Tn}(x) \right], \\ J_\mu^3(x) &= \frac{\varepsilon^{ijk}\varepsilon^{imn}}{\sqrt{2}} \left[ u^{Tj}(x) C \sigma_{\mu\nu} c^k(x) \bar{d}^m(x) \gamma_5 \gamma^\nu C \bar{c}^{Tn}(x) + u^{Tj}(x) C \gamma^\nu \gamma_5 c^k(x) \bar{d}^m(x) \sigma_{\mu\nu} C \bar{c}^{Tn}(x) \right], \\ J_{\mu\nu}(x) &= \frac{\varepsilon^{ijk}\varepsilon^{imn}}{\sqrt{2}} \left[ u^{Tj}(x) C \gamma_\mu c^k(x) \bar{d}^m(x) \gamma_\nu C \bar{c}^{Tn}(x) - u^{Tj}(x) C \gamma_\nu c^k(x) \bar{d}^m(x) \gamma_\mu C \bar{c}^{Tn}(x) \right],\end{aligned}\quad (2)$$

the  $i, j, k, m, n$  are color indexes, the  $C$  is the charge conjugation matrix. Under charge conjugation (parity) transform  $\hat{C}$  ( $\hat{P}$ ), the currents  $J_\mu(x)$  and  $J_{\mu\nu}(x)$  have the properties,

$$\begin{aligned}\hat{C} J_\mu(x) \hat{C}^{-1} &= -J_\mu(x), \\ \hat{C} J_{\mu\nu}(x) \hat{C}^{-1} &= -J_{\mu\nu}(x), \\ \hat{P} J_\mu(x) \hat{P}^{-1} &= -J^\mu(\tilde{x}), \\ \hat{P} J_{\mu\nu}(x) \hat{P}^{-1} &= J^{\mu\nu}(\tilde{x}),\end{aligned}\quad (3)$$

the four vectors  $x^\mu = (t, \vec{x})$  and  $\tilde{x}^\mu = (t, -\vec{x})$ . The currents  $J_\mu^1(x)$ ,  $J_\mu^2(x)$  and  $J_\mu^3(x)$  couple potentially to the  $[uc]_S[\bar{d}\bar{c}]_A - [uc]_A[\bar{d}\bar{c}]_S$  type,  $[uc]_T[\bar{d}\bar{c}]_A - [uc]_A[\bar{d}\bar{c}]_T$  type and  $[uc]_T[\bar{d}\bar{c}]_V + [uc]_V[\bar{d}\bar{c}]_T$  type axialvector tetraquark states with  $J^{PC} = 1^{+-}$ , respectively. While the current  $J_{\mu\nu}(x)$  couples potentially to both the  $[uc]_A[\bar{d}\bar{c}]_A$  type axialvector tetraquark state with  $J^{PC} = 1^{+-}$  and vector tetraquark state with  $J^{PC} = 1^{--}$ . The tensor diquark operators also play an important role in constructing the tetraquark current operators [20]. Thereafter, we will not distinguish the positive and negative electric charge of the  $Z_c$  states, as they have degenerate masses.

At the hadronic side, we can insert a complete set of intermediate hadronic states with the same quantum numbers as the current operators  $J_\mu(x)$  and  $J_{\mu\nu}(x)$  into the correlation functions  $\Pi_{\mu\nu}(p)$  and  $\Pi_{\mu\nu\alpha\beta}(p)$  to obtain the hadronic representation [21, 22]. After isolating the ground

state contributions of the axialvector and vector tetraquark states, we obtain the results,

$$\begin{aligned}\Pi_{\mu\nu}(p) &= \frac{\lambda_Z^2}{m_Z^2 - p^2} \left( -g_{\mu\nu} + \frac{p_\mu p_\nu}{p^2} \right) + \dots \\ &= \Pi_Z(p^2) \left( -g_{\mu\nu} + \frac{p_\mu p_\nu}{p^2} \right) + \dots,\end{aligned}\quad (4)$$

$$\begin{aligned}\Pi_{\mu\nu\alpha\beta}(p) &= \frac{\tilde{\lambda}_Z^2}{m_Z^2 - p^2} (p^2 g_{\mu\alpha} g_{\nu\beta} - p^2 g_{\mu\beta} g_{\nu\alpha} - g_{\mu\alpha} p_\nu p_\beta - g_{\nu\beta} p_\mu p_\alpha + g_{\mu\beta} p_\nu p_\alpha + g_{\nu\alpha} p_\mu p_\beta) \\ &\quad + \frac{\tilde{\lambda}_Y^2}{m_Y^2 - p^2} (-g_{\mu\alpha} p_\nu p_\beta - g_{\nu\beta} p_\mu p_\alpha + g_{\mu\beta} p_\nu p_\alpha + g_{\nu\alpha} p_\mu p_\beta) + \dots \\ &= \Pi_Z(p^2) (p^2 g_{\mu\alpha} g_{\nu\beta} - p^2 g_{\mu\beta} g_{\nu\alpha} - g_{\mu\alpha} p_\nu p_\beta - g_{\nu\beta} p_\mu p_\alpha + g_{\mu\beta} p_\nu p_\alpha + g_{\nu\alpha} p_\mu p_\beta) \\ &\quad + \Pi_Y(p^2) (-g_{\mu\alpha} p_\nu p_\beta - g_{\nu\beta} p_\mu p_\alpha + g_{\mu\beta} p_\nu p_\alpha + g_{\nu\alpha} p_\mu p_\beta),\end{aligned}\quad (5)$$

where the  $Z$  denotes the axialvector tetraquark states, the  $Y$  denotes the vector tetraquark states, the pole residues  $\lambda_Z$ ,  $\tilde{\lambda}_Z$  and  $\tilde{\lambda}_Y$  are defined by

$$\begin{aligned}\langle 0 | J_\mu(0) | Z_c(p) \rangle &= \lambda_Z \varepsilon_\mu, \\ \langle 0 | J_{\mu\nu}(0) | Z_c(p) \rangle &= \tilde{\lambda}_Z \varepsilon_{\mu\nu\alpha\beta} \varepsilon^\alpha p^\beta, \\ \langle 0 | J_{\mu\nu}(0) | Y(p) \rangle &= \tilde{\lambda}_Y (\varepsilon_\mu p_\nu - \varepsilon_\nu p_\mu),\end{aligned}\quad (6)$$

$\varepsilon_{0123} = -1$ , the  $\varepsilon_\mu$  are the polarization vectors of the vector and axialvector tetraquark states with the property,

$$\sum_\lambda \varepsilon_\mu^*(\lambda, p) \varepsilon_\nu(\lambda, p) = -g_{\mu\nu} + \frac{p_\mu p_\nu}{p^2}. \quad (7)$$

The diquark-antidiquark type currents  $J_\mu(x)$  and  $J_{\mu\nu}(x)$  couple potentially to the diquark-antidiquark type tetraquark states. We can perform Fierz rearrangements to those currents both in the color and Dirac-spinor spaces to obtain a series of color singlet-singlet type currents, for example,

$$\begin{aligned}J_\mu^1 &= \frac{1}{2\sqrt{2}} \left\{ i\bar{c}i\gamma_5 c \bar{d}\gamma^\mu u - i\bar{c}\gamma^\mu c \bar{d}i\gamma_5 u + \bar{c}u \bar{d}\gamma^\mu \gamma_5 c - \bar{c}\gamma^\mu \gamma_5 u \bar{d}c \right. \\ &\quad \left. - i\bar{c}\gamma_\nu \gamma_5 c \bar{d}\sigma^{\mu\nu} u + i\bar{c}\sigma^{\mu\nu} c \bar{d}\gamma_\nu \gamma_5 u - i\bar{c}\sigma^{\mu\nu} \gamma_5 u \bar{d}\gamma_\nu c + i\bar{c}\gamma_\nu u \bar{d}\sigma^{\mu\nu} \gamma_5 c \right\},\end{aligned}\quad (8)$$

the components such as  $\bar{c}i\gamma_5 c \bar{d}\gamma^\mu u$ ,  $\bar{c}\gamma^\mu c \bar{d}i\gamma_5 u$ , etc couple potentially to the meson-meson pairs or molecular states.

However, we should be careful in performing the Fierz rearrangements, the rearrangements in the color and Dirac-spinor spaces are highly non-trivial, the scenarios of the tetraquark states and molecular states are quite different.

According to the arguments of Selem and Wilczek, a diquark-antidiquark type tetraquark can be plausibly described by two diquarks in a double well potential separated by a barrier [23]. At long distances, the diquark and antidiquark serve as point color charges, and attract each other strongly just as in the quark-antiquark system. However, at shorter distances, the attractions between quarks and antiquarks reduce the binding energy of the diquarks and tend to destroy the diquarks. Those effects (beyond the naive one-gluon exchange force) increase at decreasing distance and produce a repulsion between diquark and antidiquark, if large enough, it will lead to a barrier between the diquark and antidiquark [24]. The double well potential separated by a barrier can give successful descriptions of the tetraquark states [24].

While in the dynamical picture of the tetraquark states, the large spatial separation between the diquark and antidiquark leads to small wave-function overlap between the quark-antiquark pair [25], the rearrangements in the color and Dirac-spinor spaces are highly suppressed.

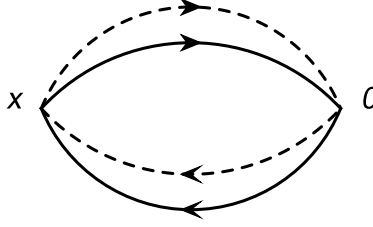


Figure 1: The Feynman diagram of the lowest order contributions for the diquark-antidiquark type currents, where the solid lines and dashed lines denote the light quarks and heavy quarks, respectively.

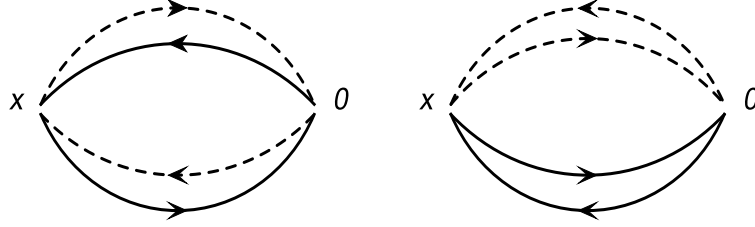


Figure 2: The Feynman diagrams of the lowest order contributions for the color singlet-singlet type currents, where the solid lines and dashed lines denote the light quarks and heavy quarks, respectively.

It is difficult to account for the non-local effects between the diquark and antidiquark pair in the currents  $J_\mu(x)$  and  $J_{\mu\nu}(x)$  directly, for example, the current  $J_\mu^1(x)$  can be modified to

$$J_\mu^1(x, \epsilon) = \frac{\epsilon^{ijk}\epsilon^{imn}}{\sqrt{2}} \left[ u^{Tj}(x) C \gamma_5 c^k(x) \bar{d}^m(x + \epsilon) \gamma_\mu C \bar{c}^{Tn}(x + \epsilon) - u^{Tj}(x) C \gamma_\mu c^k(x) \bar{d}^m(x + \epsilon) \right. \\ \left. \gamma_5 C \bar{c}^{Tn}(x + \epsilon) \right], \quad (9)$$

to account for the non-locality by adding a finite  $\epsilon$ , but it is difficult to deal with the finite  $\epsilon$  in carrying out the operator product expansion, we have to take the limit  $\epsilon \rightarrow 0$ . However, we should not take it for granted that the diquark-antidiquark type currents can be rearranged freely to a series of color singlet-singlet type currents, which couple potentially to the meson-meson pairs or molecular states.

The lowest order contributions in the correlation functions for the diquark-antidiquark type tetraquark currents can be described by the Feynman diagram shown in Fig.1. The corresponding lowest order contributions in the correlation functions for the color singlet-singlet type tetraquark currents can be described by the Feynman diagrams shown in Fig.2. The Feynman diagram shown in Fig.1 cannot be factorized into the two Feynman diagrams shown in Fig.2 freely due to the barrier (or spatial separation) between the diquark and antidiquark [24, 25]. When a quark (antiquark) in the diquark (antidiquark) penetrates the barrier, the Feynman diagram shown in Fig.1 is factorizable. In this case, the non-factorizable diagrams start at the order  $\mathcal{O}(\alpha_s^2)$  [26].

When the quark or antiquark penetrates the barrier, we can perform the Fierz rearrangements, and study the effects of the scattering states. In the following, we study the contributions of the

intermediate meson-loops to the correlation function  $\Pi_{\mu\nu}(p)$  for the current  $J_\mu^1(x)$  as an example,

$$\begin{aligned}
\Pi_{\mu\nu}(p) &= -\frac{\hat{\lambda}_Z^2}{p^2 - \widehat{M}_Z^2} \tilde{g}_{\mu\nu}(p) - \frac{\hat{\lambda}_Z}{p^2 - \widehat{M}_Z^2} \tilde{g}_{\mu\alpha}(p) \Sigma_{DD^*}(p) \tilde{g}^{\alpha\beta}(p) \tilde{g}_{\beta\nu}(p) \frac{\hat{\lambda}_Z}{p^2 - \widehat{M}_Z^2} \\
&\quad - \frac{\hat{\lambda}_Z}{p^2 - \widehat{M}_Z^2} \tilde{g}_{\mu\alpha}(p) \Sigma_{J/\psi\pi}(p) \tilde{g}^{\alpha\beta}(p) \tilde{g}_{\beta\nu}(p) \frac{\hat{\lambda}_{X/Z}}{p^2 - \widehat{M}_Z^2} + \cdots, \\
&= -\frac{\hat{\lambda}_Z^2}{p^2 - \widehat{M}_Z^2 - \Sigma_{DD^*}(p) - \Sigma_{J/\psi\pi}(p) + \cdots} \tilde{g}_{\mu\nu}(p) + \cdots,
\end{aligned} \tag{10}$$

where

$$\begin{aligned}
\Sigma_{DD^*}(p) &= i \int \frac{d^4q}{(2\pi)^4} \frac{G_{ZDD^*}^2}{[q^2 - M_D^2][(p-q)^2 - M_{D^*}^2]}, \\
\Sigma_{J/\psi\pi}(p) &= i \int \frac{d^4q}{(2\pi)^4} \frac{G_{ZJ/\psi\pi}^2}{[q^2 - M_{J/\psi}^2][(p-q)^2 - M_\pi^2]},
\end{aligned} \tag{11}$$

$\tilde{g}_{\mu\nu}(p) = -g_{\mu\nu} + \frac{p_\mu p_\nu}{p^2}$ , the  $G_{ZDD^*}$  and  $G_{ZJ/\psi\pi}$  are hadronic coupling constants, the  $\hat{\lambda}_Z$  and  $\widehat{M}_Z$  are bare objects to absorb the divergences in the self-energies  $\Sigma_{DD^*}(p)$ ,  $\Sigma_{J/\psi\pi}(p)$ , etc. The renormalized self-energies contribute a finite imaginary part to modify the dispersion relation,

$$\Pi_{\mu\nu}(p) = -\frac{\lambda_Z^2}{p^2 - M_Z^2 + i\sqrt{p^2}\Gamma(p^2)} \tilde{g}_{\mu\nu}(p) + \cdots, \tag{12}$$

the physical width  $\Gamma_{Z_c(3900)}(M_Z^2) = (46 \pm 10 \pm 20) \text{ MeV}$  [4] (or  $(28.2 \pm 2.6) \text{ MeV}$  [9]), the zero width approximation in the hadronic spectral densities works well [27]. In this article, we neglect the contributions of the scattering states or meson-meson pairs, the predictions are still robust.

We carry out the operator product expansion up to the vacuum condensates of dimension 10 in a consistent way, and take into account the vacuum condensates which are the vacuum expectations of the operators of the orders  $\mathcal{O}(\alpha_s^k)$  with  $k \leq 1$ , then obtain the QCD spectral densities through dispersion relation. Now we take the quark-hadron duality below the continuum thresholds  $s_0$  and perform Borel transform with respect to the variable  $P^2 = -p^2$  to obtain the QCD sum rules:

$$\lambda_Z^2 \exp\left(-\frac{M_Z^2}{T^2}\right) = \int_{4m_c^2}^{s_0} ds \rho(s) \exp\left(-\frac{s}{T^2}\right), \tag{13}$$

$$\rho(s) = \rho_0(s) + \rho_3(s) + \rho_4(s) + \rho_5(s) + \rho_6(s) + \rho_7(s) + \rho_8(s) + \rho_{10}(s), \tag{14}$$

$\lambda_Z = \tilde{\lambda}_Z M_Z$ , the  $T^2$  is the Borel parameter, the subscripts  $i$  in the QCD spectral densities  $\rho_i(s)$  denote the dimensions of the vacuum condensates,

$$\begin{aligned}
\rho_3(s) &\propto \langle \bar{q}q \rangle, \\
\rho_4(s) &\propto \left\langle \frac{\alpha_s GG}{\pi} \right\rangle, \\
\rho_5(s) &\propto \langle \bar{q}g_s \sigma G q \rangle, \\
\rho_6(s) &\propto \langle \bar{q}q \rangle^2, 4\pi\alpha_s \langle \bar{q}q \rangle^2, \\
\rho_7(s) &\propto \langle \bar{q}q \rangle \left\langle \frac{\alpha_s GG}{\pi} \right\rangle, \\
\rho_8(s) &\propto \langle \bar{q}q \rangle \langle \bar{q}g_s \sigma G q \rangle, \\
\rho_{10}(s) &\propto \langle \bar{q}g_s \sigma G q \rangle^2, \langle \bar{q}q \rangle^2 \left\langle \frac{\alpha_s GG}{\pi} \right\rangle,
\end{aligned} \tag{15}$$

the lengthy expressions of the QCD spectral densities are neglected for simplicity. For the technical details, one can consult Ref.[28]. For the currents  $J_\mu^1(x)$  and  $J_{\mu\nu}(x)$ , one can consult Refs.[19, 28] for the explicit expressions of the QCD spectral densities. In this work, we recalculate those QCD spectral densities, and use the formula  $t_{ij}^a t_{mn}^a = -\frac{1}{6}\delta_{ij}\delta_{mn} + \frac{1}{2}\delta_{jm}\delta_{in}$  with  $t^a = \frac{\lambda^a}{2}$  to deal with the high dimensional vacuum condensates, where the  $\lambda^a$  is the Gell-Mann matrix. This routine leads to slight but neglectful differences compared to the old calculations. For the currents  $J_\mu^2(x)$  and  $J_\mu^3(x)$ , we neglect the tiny contributions of the  $4\pi\alpha_s\langle\bar{q}q\rangle^2$ , which originate from the terms like  $\langle\bar{q}_j\gamma_\mu q_i g_s D_\nu G_{\alpha\beta}^a t_{mn}^a\rangle$ .

We derive Eq.(13) with respect to  $\tau = \frac{1}{T^2}$ , then eliminate the pole residues  $\lambda_Z$  to obtain the QCD sum rules for the masses,

$$M_Z^2 = -\frac{\int_{4m_c^2}^{s_0} ds \frac{d}{d\tau} \rho(s) e^{-\tau s}}{\int_{4m_c^2}^{s_0} ds \rho(s) e^{-\tau s}}. \quad (16)$$

Thereafter, we will refer the QCD sum rules in Eq.(13) and Eq.(16) as QCDSR I.

If we take into account the contributions of the first radial excited states  $Z'_c$  at the hadronic side, we can obtain the QCD sum rules,

$$\lambda_Z^2 \exp\left(-\frac{M_Z^2}{T^2}\right) + \lambda_{Z'}^2 \exp\left(-\frac{M_{Z'}^2}{T^2}\right) = \int_{4m_c^2}^{s'_0} ds \rho(s) \exp\left(-\frac{s}{T^2}\right), \quad (17)$$

where the  $s'_0$  is continuum threshold parameter, then we introduce the notations  $\tau = \frac{1}{T^2}$ ,  $D^n = \left(-\frac{d}{d\tau}\right)^n$ , and use the subscripts 1 and 2 to denote the ground state  $Z_c$  and the first radial excited state  $Z'_c$  respectively for simplicity. We rewrite the QCD sum rules as

$$\lambda_1^2 \exp(-\tau M_1^2) + \lambda_2^2 \exp(-\tau M_2^2) = \Pi_{QCD}(\tau), \quad (18)$$

here we add the subscript  $QCD$  to denote the QCD side. We derive the QCD sum rules in Eq.(18) with respect to  $\tau$  to obtain

$$\lambda_1^2 M_1^2 \exp(-\tau M_1^2) + \lambda_2^2 M_2^2 \exp(-\tau M_2^2) = D\Pi_{QCD}(\tau). \quad (19)$$

From Eqs.(18)-(19), we obtain the QCD sum rules,

$$\lambda_i^2 \exp(-\tau M_i^2) = \frac{(D - M_j^2) \Pi_{QCD}(\tau)}{M_i^2 - M_j^2}, \quad (20)$$

where  $i \neq j$ . Now we derive the QCD sum rules in Eq.(20) with respect to  $\tau$  to obtain

$$\begin{aligned} M_i^2 &= \frac{(D^2 - M_j^2 D) \Pi_{QCD}(\tau)}{(D - M_j^2) \Pi_{QCD}(\tau)}, \\ M_i^4 &= \frac{(D^3 - M_j^2 D^2) \Pi_{QCD}(\tau)}{(D - M_j^2) \Pi_{QCD}(\tau)}. \end{aligned} \quad (21)$$

The squared masses  $M_i^2$  satisfy the equation,

$$M_i^4 - bM_i^2 + c = 0, \quad (22)$$

where

$$\begin{aligned} b &= \frac{D^3 \otimes D^0 - D^2 \otimes D}{D^2 \otimes D^0 - D \otimes D}, \\ c &= \frac{D^3 \otimes D - D^2 \otimes D^2}{D^2 \otimes D^0 - D \otimes D}, \\ D^j \otimes D^k &= D^j \Pi_{QCD}(\tau) D^k \Pi_{QCD}(\tau), \end{aligned} \quad (23)$$

$i = 1, 2, j, k = 0, 1, 2, 3$ . We solve the equation to obtain two solutions [15],

$$M_1^2 = \frac{b - \sqrt{b^2 - 4c}}{2}, \quad (24)$$

$$M_2^2 = \frac{b + \sqrt{b^2 - 4c}}{2}. \quad (25)$$

Thereafter, we will refer the QCD sum rules in Eq.(17) and Eqs.(24)-(25) as QCDSR II. In the QCDSR II, only one solution satisfies the energy scale formula  $\mu = \sqrt{M_{X/Y/Z}^2 - (2\mathbb{M}_c)^2}$  if the energy scales of the QCD spectral densities are specified, the other solution is discarded. In this article, we retain the mass  $M_2$  ( $M_{Z'}$ ) and discard the mass  $M_1$  ( $M_Z$ ).

### 3 Numerical results and discussions

We take the vacuum condensates to be the standard values  $\langle \bar{q}q \rangle = -(0.24 \pm 0.01 \text{ GeV})^3$ ,  $\langle \bar{q}g_s \sigma G q \rangle = m_0^2 \langle \bar{q}q \rangle$ ,  $m_0^2 = (0.8 \pm 0.1) \text{ GeV}^2$ ,  $\langle \frac{\alpha_s GG}{\pi} \rangle = (0.33 \text{ GeV})^4$  at the energy scale  $\mu = 1 \text{ GeV}$  [21, 22, 29], and take the  $\overline{M}\overline{S}$  mass  $m_c(m_c) = (1.275 \pm 0.025) \text{ GeV}$  from the Particle Data Group [9]. Moreover, we take into account the energy-scale dependence of the quark condensate, mixed quark condensate and  $\overline{M}\overline{S}$  mass,

$$\begin{aligned} \langle \bar{q}q \rangle(\mu) &= \langle \bar{q}q \rangle(Q) \left[ \frac{\alpha_q(Q)}{\alpha_q(\mu)} \right]^{\frac{12}{33-2n_f}}, \\ \langle \bar{q}g_s \sigma G q \rangle(\mu) &= \langle \bar{q}g_s \sigma G q \rangle(Q) \left[ \frac{\alpha_s(Q)}{\alpha_s(\mu)} \right]^{\frac{2}{33-2n_f}}, \\ m_c(\mu) &= m_c(m_c) \left[ \frac{\alpha_s(\mu)}{\alpha_s(m_c)} \right]^{\frac{12}{33-2n_f}}, \\ \alpha_s(\mu) &= \frac{1}{b_0 t} \left[ 1 - \frac{b_1 \log t}{b_0^2 t} + \frac{b_1^2 (\log^2 t - \log t - 1) + b_0 b_2}{b_0^4 t^2} \right], \end{aligned} \quad (26)$$

where  $t = \log \frac{\mu^2}{\Lambda^2}$ ,  $b_0 = \frac{33-2n_f}{12\pi}$ ,  $b_1 = \frac{153-19n_f}{24\pi^2}$ ,  $b_2 = \frac{2857 - \frac{5033}{9}n_f + \frac{325}{27}n_f^2}{128\pi^3}$ ,  $\Lambda = 210 \text{ MeV}$ ,  $292 \text{ MeV}$  and  $332 \text{ MeV}$  for the flavors  $n_f = 5, 4$  and  $3$ , respectively [9, 30], and evolve all the input parameters to the optimal energy scales  $\mu$  with  $n_f = 4$  to extract the tetraquark masses.

The Okubo-Zweig-Iizuka supper-allowed decays

$$\begin{aligned} Z_c &\rightarrow J/\psi \pi, \\ Z'_c &\rightarrow \psi' \pi \\ Z''_c &\rightarrow \psi'' \pi, \end{aligned} \quad (27)$$

are expected to take place easily. The energy gaps maybe have the relations  $M_{Z'} - M_Z = m_{\psi'} - m_{J/\psi}$  and  $M_{Z''} - M_{Z'} = m_{\psi''} - m_{\psi'}$ . The charmonium masses are  $m_{J/\psi} = 3.0969 \text{ GeV}$ ,  $m_{\psi'} = 3.686097 \text{ GeV}$  and  $m_{\psi''} = 4.039 \text{ GeV}$  from the Particle Data Group [9],  $m_{\psi'} - m_{J/\psi} = 0.59 \text{ GeV}$ ,  $m_{\psi''} - m_{J/\psi} = 0.94 \text{ GeV}$ , we can tentatively choose the continuum threshold parameters as  $\sqrt{s_0} = M_Z + 0.59 \text{ GeV}$  and  $\sqrt{s'_0} = M_Z + 0.95 \text{ GeV}$  and vary the continuum threshold parameters and Borel parameters to satisfy the following four criteria:

1. Pole dominance at the phenomenological side;
2. Convergence of the operator product expansion;
3. Appearance of the Borel platforms;
4. Satisfying the energy scale formula,

via try and error, and obtain the Borel windows, continuum threshold parameters, ideal energy scales of the QCD spectral densities, and pole contributions of the ground states for the QCDSR I, see Table 1. The corresponding parameters for the QCDSR II are shown in Table 2. In this article, we take the energy scale formula  $\mu = \sqrt{M_{X/Y/Z}^2 - (2\mathbb{M}_c)^2}$  with the effective  $c$ -quark mass  $\mathbb{M}_c$  as a constraint [16]. The energy scale formula can enhance the pole contributions remarkably and improve the convergent behaviors of the operator product expansion, and works well for both the tetraquark states and pentaquark states [31].

From Table 1 and Table 2, we can see that the contributions of the ground states are about (40 – 60)% for the QCDSR I, the contributions of the ground states plus the first radial excited states are about (70 – 80)% for the QCDSR II, the pole dominance criterion is well satisfied. In the QCDSR II, the contributions of the ground states are about (30 – 45)%, which are much less than the corresponding ground state contributions in the QCDSR I, for the ground state masses and pole residues, we prefer the predictions from the QCDSR I. In calculations, we observe that the contributions of the vacuum condensates of dimension 10 are of percent level at the Borel widows for both the QCDSR I and QCDSR II, the operator product expansion is well convergent.

Now we take into account the uncertainties of the input parameters, and obtain the masses and pole residues of the ground states  $Z_c$  and the first radial excited states  $Z'_c$ , which are shown in Table 3 and Table 4. From the Tables, we can see that the ground state masses from the QCDSR I and the radial excited state masses from the QCDSR II satisfy the energy scale formula  $\mu = \sqrt{M_{X/Y/Z}^2 - (2\mathbb{M}_c)^2}$ , where the updated effective  $c$ -quark mass  $\mathbb{M}_c = 1.82 \text{ GeV}$  is taken [19]. In Table 4, we also present the central values of the ground state masses and pole residues extracted from the QCDSR II at the ideal energy scales shown in Table 1. From Table 4, we can see that the ground state masses cannot satisfy the energy scale formula, so we will discard those values. This is the shortcoming of the QCDSR II.

In Fig.3, we plot the ground state masses from the QCDSR I and the first radial excited state masses from the QCDSR II with variations of the Borel parameters at much larger ranges than the Borel windows shown in Table 1 and Table 2. From the figure, we can see that there appear very flat platforms in the Borel windows for the  $[uc]_S[\bar{d}\bar{c}]_A - [uc]_A[\bar{d}\bar{c}]_S$  type,  $[uc]_T[\bar{d}\bar{c}]_A - [uc]_A[\bar{d}\bar{c}]_T$  type and  $[uc]_A[\bar{d}\bar{c}]_A$  type axialvector tetraquark states. For the  $[uc]_T[\bar{d}\bar{c}]_V + [uc]_V[\bar{d}\bar{c}]_T$  type tetraquark state, we only plot the ground state mass, as the ground state mass is large enough. From the figure, we can see that the platform in the Borel window is not flat enough, at the region  $T^2 < 3.6 \text{ GeV}^2$ , the mass increases monotonously and quickly with increase of the Borel parameter, the platform appears approximately only at the region  $T^2 > 3.6 \text{ GeV}^2$ .

The predicted mass  $M_Z = 3.90 \pm 0.08 \text{ GeV}$  for the ground state  $[uc]_S[\bar{d}\bar{c}]_A - [uc]_A[\bar{d}\bar{c}]_S$  tetraquark state is in excellent agreement with the experimental data  $M_{Z(3900)} = (3899.0 \pm 3.6 \pm 4.9) \text{ MeV}$  from the BESIII collaboration [4], which supports assigning the  $Z_c(3900)$  to be the ground state  $[uc]_S[\bar{d}\bar{c}]_A - [uc]_A[\bar{d}\bar{c}]_S$  tetraquark state with  $J^{PC} = 1^{+-}$  [28]. In Ref.[32], we study the two-body strong decays  $Z_c^+(3900) \rightarrow J/\psi\pi^+, \eta_c\rho^+, D^+\bar{D}^{*0}, \bar{D}^0 D^{*+}$  with the QCD sum rules based on solid quark-hadron duality by taking into account both the connected and disconnected Feynman diagrams, and obtain the total width  $\Gamma_{Z_c} = 54.2 \pm 29.8 \text{ MeV}$ , which is consistent with the experimental data  $(46 \pm 10 \pm 20) \text{ MeV}$  considering the uncertainties [4].

The predicted mass  $M_Z = 4.47 \pm 0.09 \text{ GeV}$  for the first radial excited  $[uc]_S[\bar{d}\bar{c}]_A - [uc]_A[\bar{d}\bar{c}]_S$  tetraquark state is in excellent agreement with the experimental data  $M_{Z(4430)} = (4475 \pm 7_{-25}^{+15}) \text{ MeV}$  from the LHCb collaboration [10], which supports assigning the  $Z_c(4430)$  to be the first radial excited  $[uc]_S[\bar{d}\bar{c}]_A - [uc]_A[\bar{d}\bar{c}]_S$  tetraquark state with  $J^{PC} = 1^{+-}$ . We can study its two-body strong decays with the three-point QCD sum rules to make more reasonable assignment.

The predicted mass  $M_Z = 4.01 \pm 0.09 \text{ GeV}$  for the ground state  $[uc]_T[\bar{d}\bar{c}]_A - [uc]_A[\bar{d}\bar{c}]_T$  tetraquark state and  $M_Z = 4.00 \pm 0.09 \text{ GeV}$  for the ground state  $[uc]_A[\bar{d}\bar{c}]_A$  tetraquark state are both in excellent agreement with the experimental data  $M_{Z(4020/4025)} = (4026.3 \pm 2.6 \pm 3.7) \text{ MeV}$  [7] and  $(4022.9 \pm 0.8 \pm 2.7) \text{ MeV}$  [8] from the BESIII collaboration. There are two axialvector tetraquark state candidates with  $J^{PC} = 1^{+-}$  for the  $Z_c(4020)$ . Again the two-body strong decays should be



$Z_c$	$T^2(\text{GeV}^2)$	$s_0$	$\mu(\text{GeV})$	pole
$[uc]_S[d\bar{c}]_A - [uc]_A[d\bar{c}]_S$	2.7 – 3.1	$(4.4 \pm 0.1 \text{ GeV})^2$	1.4	(40 – 63)%
$[uc]_T[d\bar{c}]_A - [uc]_A[d\bar{c}]_T$	3.2 – 3.6	$21.0 \pm 1.0 \text{ GeV}^2$	1.7	(40 – 60)%
$[uc]_T[d\bar{c}]_V + [uc]_V[d\bar{c}]_T$	3.7 – 4.1	$(5.25 \pm 0.10 \text{ GeV})^2$	2.9	(41 – 60)%
$[uc]_A[d\bar{c}]_A$	3.2 – 3.6	$21.0 \pm 1.0 \text{ GeV}^2$	1.7	(41 – 61)%

Table 1: The Borel parameters, continuum threshold parameters, energy scales and pole contributions for the QCDSR I.

$Z_c + Z'_c$	$T^2(\text{GeV}^2)$	$s_0$	$\mu(\text{GeV})$	pole ( $Z_c$ )
$[uc]_S[d\bar{c}]_A - [uc]_A[d\bar{c}]_S$	2.7 – 3.1	$(4.85 \pm 0.10 \text{ GeV})^2$	2.6	(72 – 88)% ((35 – 52)%)
$[uc]_T[d\bar{c}]_A - [uc]_A[d\bar{c}]_T$	3.2 – 3.6	$(4.95 \pm 0.10 \text{ GeV})^2$	2.8	(64 – 80)% ((30 – 44)%)
$[uc]_A[d\bar{c}]_A$	3.2 – 3.6	$(4.95 \pm 0.10 \text{ GeV})^2$	2.8	(64 – 81)% ((29 – 43)%)

Table 2: The Borel parameters, continuum threshold parameters, energy scales and pole contributions for the QCDSR II.

studied to make the assignment more reasonably.

The predicted mass  $M_Z = 4.60 \pm 0.09 \text{ GeV}$  for the first radial excited  $[uc]_T[d\bar{c}]_A - [uc]_A[d\bar{c}]_T$  tetraquark state and  $M_Z = 4.58 \pm 0.09 \text{ GeV}$  for the first radial excited  $[uc]_A[d\bar{c}]_A$  tetraquark state are both in excellent agreement with the experimental data  $M_{Z(4600)} = 4600 \text{ MeV}$  from the LHCb collaboration [1]. On the other hand, the predicted mass  $M_Z = 4.66 \pm 0.10 \text{ GeV}$  for the ground state  $[uc]_T[d\bar{c}]_V + [uc]_V[d\bar{c}]_T$  tetraquark state is also compatible with the experimental data  $M_{Z(4600)} = 4600 \text{ MeV}$  from the LHCb collaboration [1]. Furthermore, the decay  $Z_c(4600) \rightarrow J/\psi\pi$  can take place more easily for the ground state tetraquark state, which is consistent with the observation of the  $Z_c(4600)$  in the  $J/\psi\pi$  mass spectrum [1]. In summary, there are three axialvector tetraquark state candidates with  $J^{PC} = 1^{+-}$  for the  $Z_c(4600)$ , more experimental and theoretical works are still needed to identify the  $Z_c(4600)$  unambiguously.

In Ref.[2], we tentatively assign the  $Z_c(4600)$  to be the  $[dc]_P[\bar{u}\bar{c}]_A - [dc]_A[\bar{u}\bar{c}]_P$  type vector tetraquark state according to predicted mass  $M_Z = (4.59 \pm 0.08) \text{ GeV}$  from the QCD sum rules [33], and study its two-body strong decays  $Z_c(4600) \rightarrow J/\psi\pi, \eta_c\rho, J/\psi a_0, \chi_{c0}\rho, D^*\bar{D}^*, D\bar{D}, D^*\bar{D}$  and  $D\bar{D}^*$ , with the QCD sum rules based on solid quark-hadron duality. The large partial decay width  $\Gamma(Z_c^-(4600) \rightarrow J/\psi\pi^-) = 41.4^{+20.5}_{-14.9} \text{ MeV}$  is consistent with the observation of the  $Z_c(4600)$  in the  $J/\psi\pi^-$  mass spectrum.

$Z_c$	$M_Z(\text{GeV})$	$\lambda_Z(\text{GeV}^5)$
$[uc]_S[d\bar{c}]_A - [uc]_A[d\bar{c}]_S$	$3.90 \pm 0.08$	$(2.09 \pm 0.33) \times 10^{-2}$
$[uc]_T[d\bar{c}]_A - [uc]_A[d\bar{c}]_T$	$4.01 \pm 0.09$	$(5.96 \pm 0.94) \times 10^{-2}$
$[uc]_T[d\bar{c}]_V + [uc]_V[d\bar{c}]_T$	$4.66 \pm 0.10$	$(1.18 \pm 0.22) \times 10^{-1}$
$[uc]_A[d\bar{c}]_A$	$4.00 \pm 0.09$	$(2.91 \pm 0.46) \times 10^{-2}$

Table 3: The masses and pole residues of the ground states  $Z_c$  from the QCDSR I.

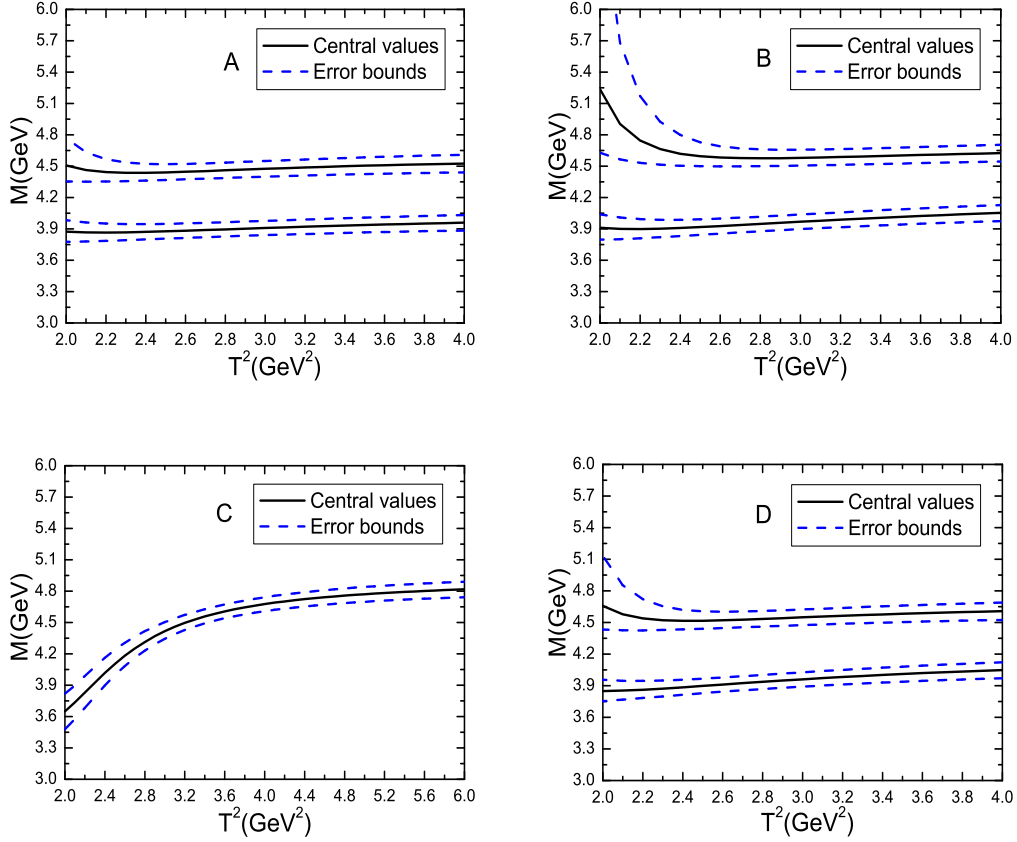


Figure 3: The masses with variations of the Borel parameters  $T^2$  for the tetraquark states, the  $A$ ,  $B$ ,  $C$  and  $D$  denote the  $[uc]_S[\bar{d}\bar{c}]_A - [uc]_A[\bar{d}\bar{c}]_S$ ,  $[uc]_T[\bar{d}\bar{c}]_A - [uc]_A[\bar{d}\bar{c}]_T$ ,  $[uc]_T[\bar{d}\bar{c}]_V + [uc]_V[\bar{d}\bar{c}]_T$  and  $[uc]_A[\bar{d}\bar{c}]_A$  tetraquark states, respectively.

$Z_c + Z'_c$	$M_Z(\text{GeV})$	$\lambda_Z(\text{GeV}^5)$	$M_{Z'}(\text{GeV})$	$\lambda_{Z'}(\text{GeV}^5)$
$[uc]_S[\bar{d}\bar{c}]_A - [uc]_A[\bar{d}\bar{c}]_S$	3.81	$1.77 \times 10^{-2}$	$4.47 \pm 0.09$	$(6.02 \pm 0.80) \times 10^{-2}$
$[uc]_T[\bar{d}\bar{c}]_A - [uc]_A[\bar{d}\bar{c}]_T$	3.78	$3.94 \times 10^{-2}$	$4.60 \pm 0.09$	$(1.35 \pm 0.18) \times 10^{-1}$
$[uc]_A[\bar{d}\bar{c}]_A$	3.73	$1.76 \times 10^{-2}$	$4.58 \pm 0.09$	$(6.55 \pm 0.85) \times 10^{-2}$

Table 4: The masses and pole residues of the ground states  $Z_c$  and the first radial excited states  $Z'_c$  from the QCDSR II.

## 4 Conclusion

In this article, we study the ground states and the first radial excited states of the  $[uc]_S[\bar{d}\bar{c}]_A - [uc]_A[\bar{d}\bar{c}]_S$  type,  $[uc]_T[\bar{d}\bar{c}]_A - [uc]_A[\bar{d}\bar{c}]_T$  type and  $[uc]_A[\bar{d}\bar{c}]_A$  type tetraquark states and the ground state  $[uc]_T[\bar{d}\bar{c}]_V + [uc]_V[\bar{d}\bar{c}]_T$  type tetraquark state with  $J^{PC} = 1^{+-}$  via the QCD sum rules in a systematic way. The predicted masses support assigning the  $Z_c(3900)$  and  $Z_c(4430)$  to be the ground state and the first radial excited state of the  $[uc]_S[\bar{d}\bar{c}]_A - [uc]_A[\bar{d}\bar{c}]_S$  tetraquark states respectively; assigning the  $Z_c(4020)$  to be the ground state  $[uc]_T[\bar{d}\bar{c}]_A - [uc]_A[\bar{d}\bar{c}]_T$  tetraquark state or  $[uc]_A[\bar{d}\bar{c}]_A$  tetraquark state; assigning the  $Z_c(4600)$  to be the first radial excited  $[uc]_T[\bar{d}\bar{c}]_A - [uc]_A[\bar{d}\bar{c}]_T$  tetraquark state or  $[uc]_A[\bar{d}\bar{c}]_A$  tetraquark state, or the ground state  $[uc]_T[\bar{d}\bar{c}]_V + [uc]_V[\bar{d}\bar{c}]_T$  tetraquark state. More experimental and theoretical works are still needed to identify the  $Z_c(4600)$  unambiguously.

## Acknowledgements

This work is supported by National Natural Science Foundation, Grant Number 11775079.

## References

- [1] R. Aaij et al, Phys. Rev. Lett. **122** (2019) 152002.
- [2] Z. G. Wang, arXiv:1901.06938.
- [3] H. X. Chen and W. Chen, Phys. Rev. **D99** (2019) 074022.
- [4] M. Ablikim et al, Phys. Rev. Lett. **110** (2013) 252001.
- [5] Z. Q. Liu et al, Phys. Rev. Lett. **110** (2013) 252002.
- [6] T. Xiao, S. Dobbs, A. Tomaradze and K. K. Seth, Phys. Lett. **B727** (2013) 366.
- [7] M. Ablikim et al, Phys. Rev. Lett. **112** (2014) 132001.
- [8] M. Ablikim et al, Phys. Rev. Lett. **111** (2013) 242001.
- [9] M. Tanabashi et al, Phys. Rev. **D98** (2018) 030001.
- [10] R. Aaij et al, Phys. Rev. Lett. **112** (2014) 222002.
- [11] M. Ablikim et al, Phys. Rev. Lett. **119** (2017) 072001.
- [12] L. Maiani, F. Piccinini, A. D. Polosa and V. Riquer, Phys. Rev. **D89** (2014) 114010.
- [13] M. Nielsen and F. S. Navarra, Mod. Phys. Lett. **A29** (2014) 1430005.
- [14] Z. G. Wang, Commun. Theor. Phys. **63** (2015) 325.
- [15] M. S. Maior de Sousa and R. Rodrigues da Silva, Braz. J. Phys. **46** (2016) 730.
- [16] Z. G. Wang, Eur. Phys. J. **C74** (2014) 2874; Z. G. Wang and T. Huang, Nucl. Phys. **A930** (2014) 63.
- [17] S. S. Agaev, K. Azizi and H. Sundu, Phys. Rev. **D96** (2017) 034026.
- [18] Z. G. Wang, Commun. Theor. Phys. **63** (2015) 466.
- [19] Z. G. Wang, Eur. Phys. J. **C76** (2016) 387.

- [20] Z. G. Wang and J. X. Zhang, Eur. Phys. J. **C76** (2016) 650. Z. G. Wang and Z. Y. Di, Eur. Phys. J. **C79** (2019) 72.
- [21] M. A. Shifman, A. I. Vainshtein and V. I. Zakharov, Nucl. Phys. **B147** (1979) 385; Nucl. Phys. **B147** (1979) 448.
- [22] L. J. Reinders, H. Rubinstein and S. Yazaki, Phys. Rept. **127** (1985) 1.
- [23] A. Selem and F. Wilczek, hep-ph/0602128.
- [24] L. Maiani, A. D. Polosa and V. Riquer, Phys. Lett. **B778** (2018) 247.
- [25] S. J. Brodsky, D. S. Hwang and R. F. Lebed, Phys. Rev. Lett. **113** (2014) 112001.
- [26] W. Lucha, D. Melikhov and H. Sazdjian, arXiv:1901.0388.
- [27] Z. G. Wang, Int. J. Mod. Phys. **A30** (2015) 1550168.
- [28] Z. G. Wang and T. Huang, Phys. Rev. **D89** (2014) 054019.
- [29] P. Colangelo and A. Khodjamirian, hep-ph/0010175.
- [30] S. Narison and R. Tarrach, Phys. Lett. **125 B** (1983) 217.
- [31] Z. G. Wang, Eur. Phys. J. **C76** (2016) 70; Z. G. Wang and T. Huang, Eur. Phys. J. **C76** (2016) 43.
- [32] Z. G. Wang and J. X. Zhang, Eur. Phys. J. **C78** (2018) 14.
- [33] Z. G. Wang, Eur. Phys. J. **C78** (2018) 518.